Physica A 183 (1992) 462–489
North-Holland

PHYSICA A

Light scattering and diffusion in suspensions of strongly charged particles at low volume fractions

Nikolai D. Denkov[1] and Dimiter N. Petsev

Laboratory of Thermodynamics and Physico-chemical Hydrodynamics, Faculty of Chemistry, University of Sofia, 1126 Sofia, Bulgaria

Received 17 July 1991
Revised manuscript received 18 November 1991

The perturbation approach of Barker and Henderson is applied to some dynamic processes in suspensions of charged Brownian particles. Analytical formulae are obtained for the first order correction of the diffusion coefficient, and sedimentation velocity, with respect to the particle volume fraction. For this purpose, the perturbation approach is combined with the theory of Felderhof. In the case of strongly charged particles (i.e. high surface potential) a simple computation procedure, involving the nonlinear Poisson–Boltzmann equation, is developed. The angular dependencies of the static and dynamic structure factors are also examined. The perturbation method allows the derivation of analytical formulae for the latter, from the general expressions of Ackerson, and Pusey and Tough. Some comparisons with numerical calculations are presented. Light scattering experiments were performed, and are analyzed by means of the proposed model.

1. Introduction

The statistical mechanical properties of a colloidal suspension, both equilibrium and nonequilibrium, depend on the particle concentration due to interparticle interactions. The equilibrium characteristics of a colloidal system, such as osmotic pressure and static structure factor, may be due to hard sphere, Coulombic, van der Waals or some other type of particle interactions [1, 2], while the dynamic properties (diffusion, sedimentation, and viscosity) include hydrodynamic interactions as well [3–7].

The Brownian motion of noninteracting colloidal particles has been studied long ago, starting with the pioneering work of Einstein [8]. A general approach for treatment of a suspension of interacting Brownian particles was developed

[1] To whom correspondence should be addressed.

by Batchelor [5, 6] and Felderhof [4, 9–12]. These authors presented the first order correction terms for the sedimentation and diffusion coefficients of hard spheres as a sum of different contributions, expressed as integrals over the radial distribution function of the particles. The final results for pure hard sphere interactions, stemming from both theoretical approaches [6, 10], coincide. The experimental verification, performed with uncharged spherical particles, also confirms the theoretical predictions [7, 13, 14]. Explicit theoretical expressions for the diffusion and sedimentation of particles, including short range attraction, are also available [5, 15]. They were used in the interpretation of dynamic light scattering (DLS) data for microemulsions [15].

Some numerical calculations, concerning the diffusion in colloidal systems with screened Coulomb interactions were performed by Ohtsuki and Okano [16]. Analytical models were also developed, based on the concept of an effective hard sphere (EHS) radius, which is due to the electrostatic repulsive forces (see e.g. the review article of Pusey and Tough [3], the monograph of Russel et al. [7] and also the recent publication of Cichocki and Felderhof [17]). However, the EHS approach introduces parameters which have not been explicitly related to the basic quantities characterizing a colloidal suspension as: particle charge, potential and radius, concentration of microions, dielectric constant of the solvent, and temperature. Such an analysis, concerning weakly charged Brownian particles, was performed recently [18]. The theory predicts [3, 17, 18] that in most cases the near field hydrodynamics contributions can be entirely neglected, and only the virial osmotic and far field hydrodynamic Oseen terms are important.

The structure and diffusivity of a suspension of interacting Brownian particles are closely related to the light scattering phenomena, occurring in such systems. For both methods, static (SLS) and dynamic (DLS) light scattering, the general theoretical results are expressed as integrals over the equilibrium radial distribution function $g(r)$ (cf. e.g. refs. [3, 4]). The simplest case is that of particles with low surface potential and charge. Then, the exponential radial distribution function and the Poisson–Boltzmann equation can be linearized and different statistical mechanical quantities can be obtained in an analytical form [18, 19]. Most of the real systems (micelles, latexes), however, are strongly charged, and for quantitative treatment, the nonlinear Poisson–Boltzmann equation (PBE) should be used. The use of the linear PBE in these cases cannot give a proper relation between the radial distribution function and the particle charge, or potential [20].

For treatment of small angle neutron scattering results from micellar solutions, the theory of Hayter and Penfold [21] and Hansen and Hayter [22] for calculation of the static structure factor of the system was proposed. This method is known as rescaled mean spherical approximation (RMSA). It yields

a good description of the static structure factor even for strongly charged particles and finite concentrations, but the calculated particle charge and potential should be regarded as effective values. Only by solving the nonlinear PBE a reliable relation between the measured quantities and the real charge (or surface potential) can be obtained [20]. The radial distribution function $g(r)$, calculated by means of RMSA or some other closures such as the hypernetted chain or Rogers–Young, can be used for numerical evaluation of the dynamic properties of colloidal suspensions [23, 24].

In the present study we propose an approach for calculating the dynamic properties of strongly charged particles, based on the perturbation theory of Barker and Henderson [25]. The radial distribution function we used allows obtaining not only the static structure factor, but also analytical expressions for the diffusion coefficient and sedimentation velocity of strongly charged particles. The angular dependence of the effective diffusion coefficient, measured by DLS, is also appropriately analyzed in terms of the present model. Explicit relations between the measured quantities and the charge (or potential) of the particles and ionic concentration are obtained, using the nonlinear PBE. Only systems at low volume fraction are considered, but the generalization for higher concentration of the particles is straightforward. We will not account for the van der Waals attraction between the particles, because it can be entirely neglected in charged suspensions with not very high concentration of added electrolyte [1, 2].

The paper is organized as follows: the next section presents the derivation of an approximate expression for the radial distribution function of charged particles consisting of two parts: one corresponding to the *reference* system of effective hard spheres (RHS) and second, accounting for the long range electrostatic *perturbation* (ELP); in section 3 this function is used for calculation of the static structure factor; the treatment of the diffusion is performed in section 4 and of the DLS in section 5; an interpretation of illustrative DLS experiment is performed in section 6; the concluding remarks are summarized in section 7.

2. Pair interactions in suspensions of charged particles

2.1. Perturbation approach for determining the radial distribution function

The knowledge of the radial distribution function $g(r)$ is of principal importance for obtaining both equilibrium (see section 3), and nonequilibrium (see sections 4 and 5) statistical mechanical properties of a given system. We can write $g(r)$ in terms of the pair potential of the mean force $W(r)$ [19, 20]:

$$g(r) = \exp\left(-\frac{W(r)}{kT}\right), \tag{2.1}$$

where kT is the thermal energy.

For weakly charged particles, with radius a, and charge number z_0, the exponential in eq. (2.1) can be linearized, and the result reads [18]

$$g(r) = \begin{cases} 0, & r \leqslant a, \\ 1 - \dfrac{(z_0 e)^2}{\varepsilon kT} \dfrac{e^{2\kappa a}}{(1+\kappa a)^2} \dfrac{e^{-\kappa r}}{r}, & r > a, \end{cases} \tag{2.2}$$

e is the elementary charge, ε is the dielectric constant of the disperse medium, and κ is the screening parameter, defined by

$$\kappa^2 = \frac{4\pi e^2}{\varepsilon kT} \sum_i n_i z_i^2, \tag{2.3}$$

where n_i, and z_i are the microion mean concentration and charge number, respectively [20].

In the case of strongly interacting particles, $g(r)$ (see eq. (2.1)) cannot be linearized, and the exact analytical calculation of quantities, as structure factors, virial coefficients, or diffusivities is impossible. In order to overcome this problem, we follow the concept of Barker and Henderson [25, 26] for presenting $g(r)$ as a sum of a reference and perturbation terms:

$$g(r) = g_0(r) + \sum_{n=1}^{\infty} g_n(r). \tag{2.4}$$

According to refs. [25, 26], the first order perturbation is given by the following expression:

$$g(r) \approx g_0(r) - g_0(r) \frac{W_1(r)}{kT}. \tag{2.5}$$

Eq. (2.5) presents the splitting of $g(r)$ into reference and perturbation parts, where W_1 is the perturbation part of the potential of mean force.

For electrostatically repelling particles, the pair interaction potential $W(r)$ can be split into reference hard sphere (RHS), and electrostatic perturbation (ELP) parts, in the manner proposed by Barker and Henderson [25, 26], and Levesque and Verlet [27]:

$$W(r) = W^{\mathrm{RHS}} + W^{\mathrm{ELP}}, \tag{2.6}$$

where

$$W^{\mathrm{RHS}}(r) = \begin{cases} W(r), & r \leq \sigma, \\ 0, & r > \sigma, \end{cases} \tag{2.7}$$

and

$$W_1 \equiv W^{\mathrm{ELP}}(r) = \begin{cases} 0, & r < \sigma, \\ W(r), & r \geq \sigma. \end{cases} \tag{2.8}$$

The value of σ should be chosen in such a way, that $W^{\mathrm{ELP}}(r)/kT < 1$ for every value of r. Still, the choice is arbitrary to some extent [25, 26]. We choose the distance σ by imposing the following condition:

$$\frac{W(r=\sigma)}{kT} = \frac{1}{2}. \tag{2.9}$$

The use of eq. (2.9) for the determination of σ leads to a remarkable coincidence between the proposed perturbation model and the numerical calculations of the system properties as static structure factor (see section 3), and collective diffusion coefficient (see section 4). There is also some physical notion in the condition (2.9), defining σ as the distance at which the repulsive energy $W(r)$ equals the Brownian kinetic energy $kT/2$. In fact, the latter is responsible for the approach of two particles in absence of any external force.

In the perturbation approach σ is a finite distance and the radius of the particles of the reference system a^{RHS} is determined by the condition [19, 25, 26]:

$$a^{\mathrm{RHS}} = \tfrac{1}{2} \int_0^{\sigma} \mathrm{d}r \, [1 - g(r)]. \tag{2.10}$$

The radius of the reference hard sphere a^{RHS} is larger than the actual particle radius a, and accounts for the low probability of approaching of two spheres beyond the distance $2a^{\mathrm{RHS}}$. For diluted suspensions the radial distribution function of the reference system $g_0(r)$ is

$$g_0(r) = \begin{cases} 0, & r < 2a^{\mathrm{RHS}}, \\ 1, & r \geq 2a^{\mathrm{RHS}}. \end{cases} \tag{2.11}$$

The choice of $\sigma \to \infty$ in eq. (2.10) leads to the simple effective hard sphere (EHS) model [3, 28]:

$$g(r) = \begin{cases} 0, & r < 2a^{\mathrm{EHS}}, \\ 1, & r \geq 2a^{\mathrm{EHS}}. \end{cases} \tag{2.12}$$

This model has been widely used for obtaining analytical results for the collective diffusion coefficient of charged particles (see ref. [3], p. 146–148). As we will show below, this approach is not always appropriate for calculation of the angular dependence of the so called effective diffusion coefficient D_{EFF} [3], and the static structure factor (see sections 3 and 5).

The splitting of the radial distribution function (see eq. (2.5)) allows also to split the integrals over $g(r)$ into two parts (see also eq. (2.11)):

$$F = \int_0^\infty \mathrm{d}r\,[1 - g(r)]\,f(r) \approx \int_0^{2a^{\mathrm{RHS}}} \mathrm{d}r\,f(r) + \int_\sigma^\infty \mathrm{d}r\,\frac{W^{\mathrm{ELP}}}{kT}\,f(r) \equiv F^{\mathrm{RHS}} + F^{\mathrm{ELP}}\,, \tag{2.13}$$

where $f(r)$ and F are arbitrary functions.

Eq. (2.13) will be used in our calculations below.

2.2. Pair energy of interaction

For determination of the pair interaction energy $W(r)$ between strongly charged particles, the nonlinear PBE needs to be involved [20]:

$$\nabla^2 y = -\frac{4\pi e^2}{\varepsilon kT} \sum_i n_i z_i \exp(-z_i y)\,, \tag{2.14}$$

where $y = e\Psi(r)/kT$ is the dimensionless potential. For spherical particles eq. (2.14) cannot be solved analytically to give the potential distribution. Hence, no explicit expression for the interaction energy $W(r)$ can be obtained, but the asymptote at $r \to \infty$ is known to have a Yukawa form [20]:

$$y(r) \to \frac{e^2}{\varepsilon kT}\,\bar{y}\,\frac{\mathrm{e}^{-\kappa r}}{r}\,, \qquad \text{for } |y| \ll 1\,. \tag{2.15}$$

$\bar{y}$ is a quantity, which can be obtained exactly by numerical intergration of eq. (2.14), and matching the boundary condition at $r = a$:

$$\left[\frac{\mathrm{d}y}{\mathrm{d}r}\right]_{r=a} = -\frac{z_0 e^2}{\varepsilon kTa^2}\,. \tag{2.16}$$

From a practical viewpoint, it is convenient to perform the numerical integration of eq. (2.14), starting from a point r_∞, disposed at large distance from the particle surface ($r_\infty \gg (1 + \kappa a)/\kappa$) with boundary conditions (cf. eq. (2.15)),

$$y(r_\infty) = \frac{e^2}{\varepsilon kT}\,\bar{y}\,\frac{e^{-\kappa r_\infty}}{r_\infty}\,, \tag{2.17}$$

$$\left[\frac{dy}{dr}\right]_{r=r_\infty} = -\frac{e^2}{\varepsilon kT}\,\bar{y}\left(\kappa + \frac{1}{r_\infty}\right)\frac{e^{-\kappa r_\infty}}{r_\infty}\,. \tag{2.18}$$

If the particle charge z_0 (or potential Ψ_s) is known, $\bar{y}$ is considered as a parameter, determined by the requirement that the solution of the PBE must satisfy eq. (2.16).

For large distances, where eq. (2.15) holds, the energy of pair interaction can be expressed in the following manner [20]:

$$\frac{W(r)}{kT} = \frac{W_0}{kT}\,2a\,e^{2\kappa a}\,\frac{e^{-\kappa r}}{r}\,, \tag{2.19}$$

where

$$\frac{W_0}{kT} = \frac{e^2\bar{y}^2\,e^{-2\kappa a}}{2\varepsilon kTa}\,. \tag{2.20}$$

Combining eqs. (2.9), (2.15), (2.19), and (2.20), we obtain

$$y(\sigma/2) = \left(\frac{2e^2}{\varepsilon kT\sigma}\right)^{1/2} < \left(\frac{0.69}{a}\right)^{1/2}\,, \tag{2.21}$$

where a is expressed in nanometers. Hence, for particles with radius greater than several nanometers $|y(\sigma/2)| \ll 1$, and the effect of the nonlinearity of the PBE (eq. (2.14)) on the potential distribution $y(r)$ is significant at distances where the radial distribution function is essentially zero. For that reason we can use eqs. (2.9), (2.10), and (2.19) for calculation of the distance σ and a^{RHS}. However, *for computation of the real surface charge, or potential from the interaction energy, the nonlinear PBE should be used.*

In fig. 1, the calculated values of $\sigma/2a$ and $\gamma = a^{\mathrm{RHS}}/a$ for W_0/kT between 1 and 200, and for a set of values of κa between 0.2 and 5, are shown (see eqs. (2.1), (2.9), (2.10), and (2.19)). It can be seen that for small W_0/kT and large κa, both $\sigma/2a$ and γ tend to unity, which corresponds to pure hard sphere interaction. However, at $\kappa a \leqslant 1$ and large values of W_0/kT, $\sigma/2a$ and γ become much larger than unity.

For particles with low surface potential Ψ_s, the linear PBE can be used:

$$\nabla^2 y = \kappa^2 y\,, \tag{2.22}$$

to obtain [20]

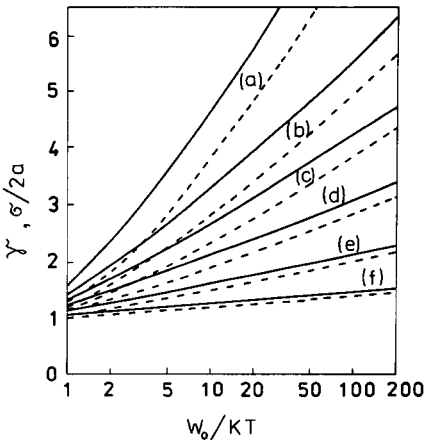

Fig. 1. $\sigma/2a$ (full curves) and γ (dashed curves) versus W_0/kT for: (a) $\kappa a = 0.2$; (b) $\kappa a = 0.4$; (c) $\kappa a = 0.6$; (d) $\kappa a = 1$; (e) $\kappa a = 2$; (f) $\kappa a = 5$.

$$y(r) = \frac{e\Psi(r)}{kT} = \frac{z_0 e^2}{\varepsilon kT} \frac{e^{\kappa a}}{1+\kappa a} \frac{e^{-\kappa r}}{r}, \tag{2.23}$$

$$z_0 e = \Psi_s \varepsilon a(1+\kappa a) \tag{2.24}$$

and

$$\frac{W_0}{kT} = \frac{(z_0 e)^2}{2\varepsilon kTa} \frac{1}{(1+\kappa a)^2}. \tag{2.25}$$

A comparison of eq. (2.25) with eq. (2.19) shows that for particles with low surface potential, the quantity W_0 presents the energy of pair interaction at the point of contact between the particles. For particles with extremely low charge number z_0 (e.g. some proteins), $W_0/kT < 1$ and eq. (2.1) can also be linearized (cf. eq. (2.2)), which leads to great simplification of any further calculations [18]. Usually this is a very drastic assumption. We should mention that even the use of the linear PBE does not necessarily give the possibility for linearization of $g(r)$.

3. Static structure factor for suspension of strongly charged colloidal particles

In this section we show how the proposed perturbation approach can be used for derivation of the static structure factor for a suspension of strongly charged Brownian particles.

The static structure factor is defined as [3, 19]

$$S(q) = 1 - \frac{3\phi}{a^3} \int_0^\infty \mathrm{d}r\, r^2 [1 - g(r)] \frac{\sin(qr)}{qr} , \tag{3.1}$$

where ϕ is the particle volume fraction and q is the magnitude of the scattering vector:

$$q = \frac{4\pi n}{\Lambda} \sin(\theta/2) , \tag{3.2}$$

n is the refractive index of the solution, Λ is the wavelength of the incident beam in vacuo and θ is the scattering angle. At $q \to 0$ we have

$$S(0) = 1 - \lambda_V \phi , \tag{3.3}$$

where λ_V is the second osmotic virial coefficient (see eq. (4.4)).

Usually, for interpretation of DLS results at low volume fractions, the EHS approach (see eq. (2.12)) is used [3, 17], which gives qualitatively correct results. In this case for $S(q)$ one obtains [17, 29]

$$S^{\mathrm{EHS}}(q) = 1 - \phi\left(\frac{24}{p^3} [\sin(\gamma^{\mathrm{EHS}} p) - \gamma^{\mathrm{EHS}} p \cos(\gamma^{\mathrm{EHS}} p)]\right) , \tag{3.4}$$

where

$$\gamma^{\mathrm{EHS}} = a^{\mathrm{EHS}}/a \quad \text{and} \quad p = 2qa , \tag{3.5}$$

γ^{EHS} is the ratio of the effective and the real hard sphere radii of the particles. In fig. 2 the EHS-approach (eq. (3.4), the dashed curve), and the result from numerical integration of eq. (3.1) together with eqs. (2.1) and (2.19), are compared. The following values for the parameters were used in the computations: radius $a = 10$ nm, screening parameter $\kappa a = 1$, and $W_0/kT = 87.3$. The value $\gamma^{\mathrm{EHS}} = 2.985$ was evaluated by means of eq. (2.10) with $\sigma \to \infty$ and eq. (3.5). The difference between the two curves is significant. For example, the value of λ_v calculated by the EHS-model is 11% lower than the exact value. Much higher is the error in the slope of the dependence of $S(q)$ on q^2 for small scattering angles – see the inset in fig. 2. It turns out that the exact value of the slope is 1.5 times higher than the calculated one by the EHS-model. These facts show that the simple EHS-model is not accurate enough to allow quantitative treatment of $S(q)$.

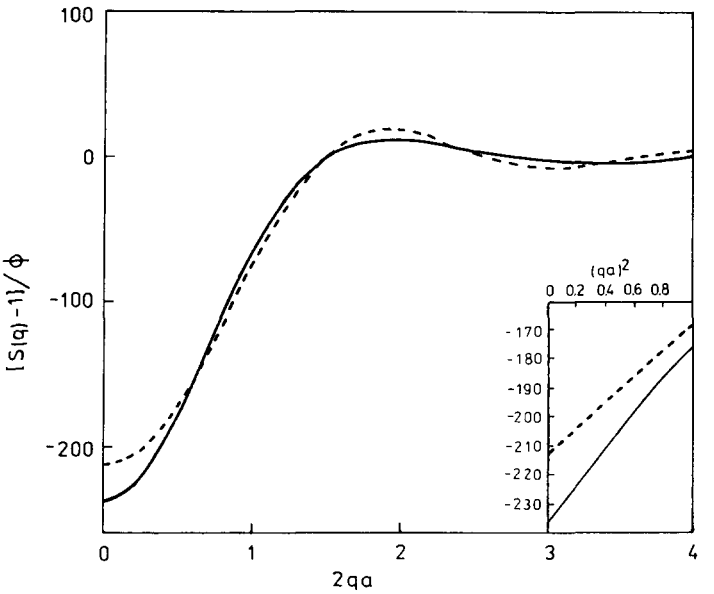

Fig. 2. Static structure factor $S(q)$ versus $2qa$. The full lines presenting the numerical calculations (eq. (3.1)) coincide with the results of the perturbation model (eq. 3.6). The dashed lines correspond to the EHS model (eq. (3.4)). The inset shows the dependence $S(q)$ vs $(qa)^2$ at small scattering angles. $a = 10$ nm, $\kappa a = 1$, and $W_0/kT = 87.3$.

Now, we can introduce into eq. (3.1), the approximate expression (2.5) for $g(r)$, obtained by the perturbation method. Splitting the integral in eq. (3.1), in the same manner as was shown above (cf. eq. (2.13)), we obtain two integrals, which can be evaluated explicitly to yield

$$S(q) = 1 - \phi\left(\frac{24}{p^3}\left[\sin(\gamma p) - \gamma p \cos(\gamma p)\right]\right.$$

$$\left. + 2\,\frac{W_0}{kT}\exp[\kappa(2a-\sigma)]\,\frac{\frac{\kappa}{q}\sin(q\sigma) + \cos(q\sigma)}{a^2(\kappa^2+q^2)}\right). \tag{3.6}$$

Hereafter we adopt, for simplicity, the notation

$$\gamma \equiv \gamma^{\mathrm{RHS}} = a^{\mathrm{RHS}}/a\,. \tag{3.7}$$

Using the above values for a, κa and W_0/kT, we obtain: $\sigma/a = 6.0547$ and $\gamma = 2.7893$. For that purpose eqs. (2.9) and (2.10) were used. The curve for $S(q)$, calculated by means of eq. (3.6), practically coincides with the full curve (the exact result) in fig. 2. The relative errors of the values of λ_V and the slope

of $S(q)$ on q^2 for small q, are less than 1%. Hence, eq. (3.6) together with eqs. (2.10), (2.19), and (3.7) can be used for accurate computation of the static structure factor at low particle concentrations. The quantity W_0 can be related to the real charge and potential of the particles by solving the nonlinear PBE – see eqs. (2.14), (2.16)–(2.18), and (2.20). With the given values of W_0/kT, a, and κa, we obtained $z_0 = 150.7$ and $e\Psi_s/kT = 3.98$.

4. First order correction of the diffusion coefficients D_C and D_S^S, and the sedimentation velocity U

Following the theoretical approach of Felderhof [4, 10], we can write

$$D_C = D_0(1 + \lambda\phi)\,, \tag{4.1}$$

where

$$\lambda = \lambda_V + \lambda_O + \lambda_A + \lambda_S + \lambda_D\,. \tag{4.2}$$

D_C is the collective diffusion coefficient which multiplies the concentration gradient in Fick's law, and D_0 is the diffusion coefficient at volume fraction $\phi \to 0$. The latter may differ from the Stokes–Einstein value [8]

$$D_{SE} = \frac{kT}{6\pi\eta a} \tag{4.3}$$

when *charged* Brownian particles are considered. The reason is the deformation of the counterion atmosphere due to the Brownian motion of the particles (see refs. [18, 30, 31]). The different contributions in eq. (4.2) are [4, 10]

$$\lambda_V = \frac{3}{a^3}\int_0^\infty \mathrm{d}r\,[1 - g(r)]r^2\,, \tag{4.4}$$

which is the second virial osmotic coefficient,

$$\lambda_O = -\frac{3}{a^2}\int_0^\infty \mathrm{d}r\,[1 - g(r)]r \tag{4.5}$$

is the Oseen term, taking into account the far field hydrodynamic contribution,

$$\lambda_A = \frac{6\pi\eta}{a^2}\int_0^\infty \mathrm{d}r\,[\alpha_{11}^{tt}(r) + 2\beta_{11}^{tt}(r)]\,g(r)\,r^2 \tag{4.6}$$

and

$$\lambda_S = \frac{6\pi\eta}{a^2} \int_0^\infty dr \left(\alpha_{12}^{tt}(r) + 2\beta_{12}^{tt}(r) - \frac{1}{2\pi\eta r} \right) g(r)\, r^2 \tag{4.7}$$

account for the near field hydrodynamics. The scalar translational mobility functions $\alpha_{1i}^{tt}(r)$ and $\beta_{1i}^{tt}(r)$ $(i = 1, 2)$ in eqs. (4.6) and (4.7) can be obtained with an arbitrary accuracy as power series expansions of the ratio a/r, by using the numerical algorithm, developed by Schmitz and Felderhof [32–34] (see also refs. [11, 12]). Thus, λ_A and λ_S can be evaluated (see tables I and II in ref. [12]):

$$\begin{aligned} \lambda_A = \frac{3}{2} \int_0^\infty dx \, [& -2.5x^{-4} + 2.25x^{-6} + 5.3334x^{-8} - 61.42x^{-10} - 94.24x^{-12} \\ & + 134.58x^{-14} - 248.46x^{-16} - 1587.4x^{-18} \\ & + 727.2x^{-20} + \mathcal{O}(x^{-22})] \, g(x)\, x^2 \end{aligned} \tag{4.8}$$

and

$$\begin{aligned} \lambda_S = \int_0^\infty dx \, [& 18.75x^{-7} - 7.5x^{-9} - 89.39x^{-11} + 215.5x^{-13} + 843.8x^{-15} \\ & + 435.9x^{-17} + 4164x^{-19} + \mathcal{O}(x^{-21})] \, g(x)\, x^2 , \end{aligned} \tag{4.9}$$

where $x = r/a$ is the dimensionless distance between the particle centers. The terms up to x^{-20} have been taken into account.

The last term in eq. (4.2),

$$\lambda_D = 1 , \tag{4.10}$$

is a force dipole part. All these quantities were evaluated for hard spheres yielding [10] $\lambda_V^{HS} = 8$, $\lambda_O^{HS} = -6$, $\lambda_A^{HS} = -1.831$, $\lambda_S^{HS} = 0.285$, and

$$D_C = D_0(1 + 1.454\phi) . \tag{4.11}$$

It was shown in ref. [10] that taking only the first term in the expansion for λ_S, one can obtain a hard sphere result ($\lambda_S = 0.293$) close to the exact asymptotic value ($\lambda_S = 0.285$). For λ_A, however, we need some higher order terms to obtain a sufficient accuracy.

For weakly charged particles, where the expression (2.2) for the radial distribution function can be adopted, the diffusion coefficients D_C and D_S^S, and the sedimentation velocity can be expressed as a sum of hard sphere and electrostatic terms: λ^{HS} and λ^{EL} [18]. Thus, for the collective diffusion coefficient D_C we have

$$D_C = D_0\left[1 + \left(1.45 + \frac{(z_0e)^2}{\varepsilon kTa}\,\frac{1}{1+\kappa a}\,\frac{3}{(\kappa a)^2}\right)\phi\right]. \tag{4.12}$$

It was shown, in ref. [18], that eq. (4.12) describes very well the experimental results of Anderson et al. [35] for the diffusion of protein molecules (bovine serum albumin), without using any adjustable parameter. The electrostatic terms λ_A^{EL} and λ_S^{EL} are neglected in eq. (4.12), because their contribution is less than 3% for any value of κa and z_0 [18]. However, for the short time self-diffusion coefficient we have [3, 10, 17]

$$D_S^S = D_0(1 + \lambda_A\phi) \tag{4.13}$$

or in the framework of the approach in ref. [18] (see also eq. (4.8)):

$$\begin{aligned} D_S^S = D_0\Big[1 - \Big(1.83 - \frac{(z_0e)^2}{\varepsilon kTa}\,\frac{e^{2\kappa a}}{(1+\kappa a)^2}\,[&0.9375\,E_3(2\kappa a) \\ &- 0.2109\,E_5(2\kappa a) - 0.125\,E_7(2\kappa a) + 0.3599\,E_9(2\kappa a) \\ &+ 0.138\,E_{11}(2\kappa a) - 0.04928\,E_{13}(2\kappa a) + 0.02275\,E_{15}(2\kappa a) \\ &+ 0.03633\,E_{17}(2\kappa a) - 0.00416\,E_{19}(2\kappa a)]\Big)\phi\Big], \end{aligned} \tag{4.14}$$

where $E_n(x)$ is an integral exponent of order n.

The sedimentation velocity U can be expressed as follows (the terms λ_A^{EL} and λ_S^{EL} are negligible again [18]):

$$U = U_0\left[1 - \left(6.55 + \frac{(z_0e)^2}{\varepsilon kTa}\,\frac{1}{(1+\kappa a)^2}\,\frac{3}{\kappa a}\right)\phi\right]. \tag{4.15}$$

U_0 is the sedimentation velocity of a single colloidal sphere.

For colloidal systems which consist of *strongly charged particles* some difficulties arise because the colloid–colloid radial distribution function cannot be linearized (see eq. (2.1) and the comments below it). Still, a hard sphere radius, corresponding to the reference system a^{RHS}, can be defined according to the procedure described in section 2. Splitting the integrals (4.4)–(4.9) (see eq. (2.13)), we can obtain a reference hard sphere (RHS), and electrostatic

perturbation (ELP) parts. In some particular cases the RHS contribution could dominate that of the electrostatic tail. However, for most real systems, the RHS, and the ELP Yukawa terms lead to comparable contributions. For such situations we can write the collective diffusion coefficient in the form (cf. eqs. (4.1) and (4.2))

$$D_C = D_0[1 + (\lambda_V + \lambda_O + \lambda_D + \lambda_A^{RHS} + \lambda_S^{RHS})\phi] , \tag{4.16}$$

where

$$\lambda_V = 8\gamma^3 + 2\frac{W_0}{kT} e^{\kappa(2a-\sigma)} \frac{3(1+\kappa\sigma)}{(\kappa a)^2} , \tag{4.17}$$

$$\lambda_O = -6\gamma^2 - 2\frac{W_0}{kT} e^{\kappa(2a-\sigma)} \frac{3}{\kappa a} , \tag{4.18}$$

$$\lambda_A^{RHS} = -\frac{15}{8\gamma} + \frac{9}{64\gamma^3} + \mathcal{O}(\gamma^{-5}) , \tag{4.19}$$

$$\lambda_S^{RHS} = \frac{75}{256\gamma^4} + \mathcal{O}(\gamma^{-6}) , \tag{4.20}$$

$$\lambda_D = 1 . \tag{4.21}$$

For not very large values of κa, when $\gamma \geq 1.2$ (see fig. 1), the terms corresponding the near field hydrodynamics can be omitted in the sum (4.16). Thus, we obtain

$$\lambda = 8\gamma^3 - 6\gamma^2 + 6\frac{W_0}{kT} e^{\kappa(2a-\sigma)} \left(\frac{(1+\kappa\sigma)}{(\kappa a)^2} - \frac{1}{\kappa a} \right) . \tag{4.22}$$

For the short time self-diffusion coefficient (cf. eq. (4.13)) the coefficient λ_A needs to be calculated:

$$\lambda_A = -\frac{15}{8\gamma} + \frac{9}{64\gamma^3} + 2\frac{W_0}{kT} e^{2\kappa a} \frac{(\kappa a)^2}{(\kappa\sigma)^2} \left(\frac{15}{4} E_3(\kappa\sigma) - \frac{27}{8} \frac{(\kappa a)^2}{(\kappa\sigma)^2} E_5(\kappa\sigma) \right) . \tag{4.23}$$

We kept only the first two terms in the expansion for the RHS and the ELP parts, but the generalization involving higher order terms is trivial. For strongly charged particles, however, the latter ones are even less important.

Finally, the sedimentation velocity can be written in the form

$$U = U_0\left[1 - \left(6\gamma^2 - 1 + \frac{15}{8\gamma} - \frac{9}{64\gamma^3} - \frac{75}{256\gamma^4} + 2\,\frac{W_0}{kT}\,e^{\kappa(2a-\sigma)}\,\frac{3}{\kappa a}\right)\phi\right]. \tag{4.24}$$

In eqs. (4.16) and (4.24), the terms λ_A^{ELP}, and λ_S^{ELP} are neglected, because their contribution in the correction term λ is less than 3% [18].

An illustration of the adequacy of the present perturbation model is given in fig. 3. The solid curve (a) presents the exact numerical calculations of λ (cf. eqs. (2.1), (2.19), (4.2) and (4.4)–(4.10)) at different values of the parameter W_0, and $\kappa a = 1$. These exact results (curve (a)) coincide entirely with those, obtained with the approximate perturbation model (eq. (4.22)). The broken curve (b) is obtained by using the EHS approach (see eq. (2.12)). The values of a^{EHS} were calculated by means of eq. (2.10) with $\sigma \to \infty$. Curve (c) in fig. 3 corresponds to the linear approximation (4.12) for weakly charged particles (see also eq. (2.25)). It is seen that the linear approximation is reasonable for $W_0/kT \leq 2$.

Another check of the proposed perturbation model (eq. (4.22)) is the comparison with the numerical calculation for the collective diffusion coefficient at different electrolyte concentrations, performed by D'Aguanno et al. [23], which is presented in fig. 4. The radius of the particles is $a = 2.5 \times 10^{-7}$ cm and the charge number is $z_0 = 20$. The solid curves are the results from ref. [23] while the broken straight lines are obtained using eqs. (4.1) and (4.22). For calculation of the values of γ and σ in eq. (4.22), we used eqs. (2.9), (2.10), (2.19), and (3.7). The values of W_0 were obtained by numerical

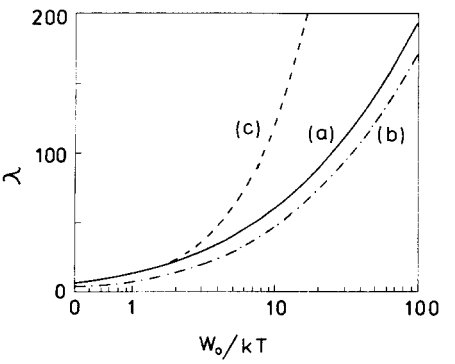

Fig. 3. First order correction of the collective diffusion coefficient λ versus the interaction parameter W_0/kT. The full line (a) presents the numerical results (eqs. (4.4)–(4.10)), coinciding with the perturbation results (eq. (4.22)). The curve (b) is obtained using the EHS model. Curve (c) is calculated from the linear model (eq. (4.12)).

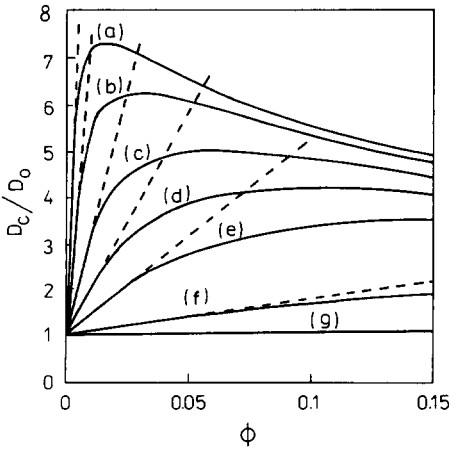

Fig. 4. Comparison between the results for the collective diffusion coefficient D_C versus ϕ from ref. [23] (full curves) with our model (eq. (4.22), dashed curves). The particle radius is $a = 2.5$ nm, charge $z_0 = 20$. The different curves refer to: (a) $\kappa a = 0.2626$; (b) $\kappa a = 0.3714$; (c) $\kappa a = 0.5872$; (d) $\kappa a = 0.8306$; (e) $\kappa a = 1.7460$; (f) $\kappa a = 2.6265$; (g) HS result.

integration of the nonlinear PBE – see eqs. (2.14), (2.16)–(2.20). It is well seen that a very good agreement at low volume fraction is reached without any adjustable parameters. The collective diffusion coefficient is seen to be very sensitive toward the electrolyte concentration (or κa), and particle volume fraction ϕ. Fig. 4 gives also some idea about the range of validity of our model for calculation of D_C at different parameters of the system (some of these parameters are summarized in table I). It is seen from fig. 4 and table I that our model is valid for $\phi^{RHS} = \phi/\gamma^3 \leq 0.1$.

Table I
Results for particles with radius $a = 2.5 \times 10^{-7}$ cm, and charge $z_0 = 20$ at several values of κa (cf. ref. [23]). The surface potential Ψ_s and the parameter W_0 are obtained by numerical integration of the nonlinear PBE (see eqs. (2.14)–(2.20)). The values of σ, γ, and λ are calculated by means of eqs. (2.9), (2.10), (3.7), and (4.22). See also fig. 4.

κa	$e\Psi_s/kT$	W_0/kT	σ/a	γ	λ
0.2626	4.05	26.6	10.73	4.62	1491
0.3714	3.67	21.6	8.31	3.61	633
0.5872	3.14	15.8	6.01	2.64	209
0.8306	2.73	12.0	4.78	2.13	92.8
1.1746	2.32	8.8	3.88	1.75	42.8
2.6265	1.45	3.6	2.64	1.23	8.8

5. Dynamic light scattering from electrostatically interacting particles

In DLS experiments one usually measures the field autocorrelation function of the scattered light [3]:

$$g^{(1)}(q,\tau) = \langle E_S(q,0)\, E_S^*(q,\tau)\rangle / \langle |E_S|^2\rangle \,, \tag{5.1}$$

where $E_S(q, t)$ is the amplitude of the electric field on the detector at the moment t, the angular brackets denote time averaging and the asterisk mean complex conjugation. q is the magnitude of the scattering vector (cf. eq. (3.2)). For a system of N identical scattering particles $g^{(1)}(q, \tau)$ can be written as

$$g^{(1)}(q,\tau) = F(q,\tau)/S(q) \,, \tag{5.2}$$

where $S(q)$ is the static structure factor and the dynamic structure factor $F(q, \tau)$ is defined by (see e.g. ref. [3]):

$$F(q,\tau) = \frac{1}{N} \sum_{k,j=1}^{N} \langle \exp\{i\boldsymbol{q}\cdot[\boldsymbol{r}_k(0) - \boldsymbol{r}_j(\tau)]\}\rangle \,. \tag{5.3}$$

Here $\boldsymbol{r}_k(t)$ is the position vector of particle k at the moment t.

Ackerson [36] and Pusey and Tough [3] showed that for a system of interacting particles an appropriate analysis can be performed in terms of the cumulant expansion:

$$\ln g^{(1)}(\tau) = \sum_n K_n \frac{(-\tau)^n}{n!} \,, \tag{5.4}$$

where K_n is the nth cumulant.

By assuming pair-wise additivity of the potential and hydrodynamic interactions between the particles, Ackerson [36] and Pusey and Tough [3] demonstrated that the first cumulant K_1 defines an effective diffusion coefficient D_{EFF}, which at low particle volume fraction is written

$$D_{EFF}(q) = \frac{K_1}{q^2} = \frac{D_0}{S(q)} [1 + \phi(\delta_O + \delta_D + \delta_A + \delta_S)] \,, \tag{5.5}$$

where ϕ is the particle volume fraction and

$$\delta_O = -\tfrac{9}{2} a^{-2} \int_0^\infty dr\, r[1 - g(r)] \left(\frac{\sin(qr)}{qr} + \frac{\cos(qr)}{(qr)^2} - \frac{\sin(qr)}{(qr)^3} \right) , \tag{5.6}$$

$$\delta_D = 1 - 3\int_0^\infty \frac{dr}{r}\,[1 - g(r)]\,j_2(qr)\,, \tag{5.7}$$

$$\delta_A = \lambda_A\,, \tag{5.8}$$

$$\delta_S = \frac{225}{4}\,a^4 \int_0^\infty \frac{dr}{r^5}\,g(r)\left(\frac{\sin(qr)}{qr} + 2\,\frac{\cos(qr)}{(qr)^2} - 2\,\frac{\sin(qr)}{(qr)^3}\right). \tag{5.9}$$

In deriving of eqs. (5.5)–(5.9) the analytical expression for the two particle mobility tensors obtained by Felderhof [9–12] were used. For the evaluation of δ_S, only the first term in the expansion (4.9) was considered. $j_2(x)$ in eq. (5.7) is the spherical Bessel function. For small values of ϕ we can write (cf. eq. (3.1))

$$D_{EFF}(q) = D_0(1 + \delta\phi)\,, \tag{5.10}$$

$$\delta = \delta_V + \delta_O + \delta_D + \delta_A + \delta_S\,, \tag{5.11}$$

where δ_V is given by

$$\delta_V = \frac{3}{a^3}\int_0^\infty dr\, r^2[1 - g(r)]\,\frac{\sin(qr)}{qr}\,. \tag{5.12}$$

The general expressions (5.5)–(5.12) give the angular dependence of the effective diffusion coefficient measured by the initial decay of the dynamic structure factor $F(q, \tau)$ in DLS experiments. At small scattering angles, where $q \to 0$, $\delta_i \to \lambda_i$ and $D_{EFF} \to D_C$.

For interpretation of the measured values of D_{EFF} and D_C in case of charged particles, one usually applies the simple EHS model (cf. eq. (2.12)). The effective radius of the charged spheres a^{EHS} is determined either via eq. (2.10) with $\sigma \to \infty$ [28] or by the expression [17]

$$a^{EHS} = \tfrac{1}{2}a(\lambda_V)^{1/3}\,, \tag{5.13}$$

where λ_V is the second osmotic virial coefficient (cf. eq. (4.4)).

Below, we apply the perturbation approach and obtain simple analytical formulae for $D_{EFF}(q)$ at small scattering angles ($qa \ll 1$). We start with the case of noncharged hard spheres because some of the results are necessary for the further consideration.

5.1. Calculation of $D_{EFF}(q)$ for a hard sphere suspension

By using the hard sphere radial distribution function (eq. (2.12) with $a^{EHS} = a$), one obtains [17]

$$\delta_V^{HS} = \frac{24}{p^3}\left[\sin(p) - p\cos(p)\right], \tag{5.14}$$

$$\delta_O^{HS} = -\frac{18}{p^3}\left[\sin(p) - p\cos(p)\right], \tag{5.15}$$

$$\delta_D^{HS} = \frac{3}{p^3}\left[\sin(p) - p\cos(p)\right], \tag{5.16}$$

$$\delta_A^{HS} = \lambda_A, \tag{5.17}$$

$$\delta_S^{HS} = -\frac{225}{224}\frac{1}{p^3}\left[\sin(p) - p\cos(p)\right] + \frac{225}{448}\left[\sin(p)\left(\frac{1}{p} - \frac{p}{12} + \frac{p^3}{24}\right) + \cos(p)\left(\frac{1}{4} - \frac{p^2}{24}\right) - \frac{p^4}{24}\,\mathrm{ci}(p)\right], \tag{5.18}$$

where $p = 2qa$ and $\mathrm{ci}(p)$ is an integral cosine function. Even for such a simple radial distribution function, the results cannot be expressed in terms of elementary mathematical functions. Much more complicated are the integrals when electrostatic repulsion must be taken into account. For that reason, asymptotic expansions of $\delta_i(q)$ for small scattering angles might be useful. The results read

$$\delta_V^{HS} = 8 - \tfrac{4}{5}p^2 + \tfrac{1}{35}p^4 + \mathcal{O}(p^6), \tag{5.19}$$

$$\delta_O^{HS} = -6 + \tfrac{3}{5}p^2 - \tfrac{3}{140}p^4 + \mathcal{O}(p^6), \tag{5.20}$$

$$\delta_D^{HS} = 1 - \tfrac{1}{10}p^2 + \tfrac{1}{280}p^4 + \mathcal{O}(p^6), \tag{5.21}$$

$$\delta_A^{HS} = \lambda_A^{HS} = -1.83, \tag{5.22}$$

$$\delta_S^{HS} = \tfrac{75}{256} - \tfrac{315}{1792}p^2 + \tfrac{75}{3584}p^4\ln(p) - \tfrac{15}{25088}p^4 + \mathcal{O}(p^6). \tag{5.23}$$

Keeping only the terms of order p^2 we obtain

$$\delta^{HS} = \lambda^{HS} - 1.903(qa)^2 + \mathcal{O}(p^4 \ln p). \tag{5.24}$$

The latter expression is compared in fig. 5 with the result obtained by Russel and Glendinning [29] for arbitrary angles by means of numerical evaluation of D_{EFF} and using the exact, numerically calculated values for the two particle mobility tensors [5]. For $qa < 0.75$ the exact results and the expansion (5.24) practically coincide. The magnitude of q in the real light scattering experiments is of the order of $10^5\,cm^{-1}$. Hence, the simple expression (5.24) can be successfully applied for uncharged particles with diameter $2a < 150$ nm.

Eqs. (5.19)–(5.23) show that for hard spheres all the contributions of the four terms δ_V, δ_O, δ_D and δ_S, in the angular dependence of D_{EFF} are significant and none of them can be neglected.

5.2. *Calculation of $D_{EFF}(q)$ for charged particles at small angles*

The expansion of the integrals in the right-hand sides of eqs. (5.6)–(5.9), and (5.12) for small values of q gives

$$\delta_V = \lambda_V - \tfrac{1}{2}(qa)^2 \int_0^\infty dx\, x^4[1 - g(x)] + \mathcal{O}(q^4a^4)\,, \tag{5.25}$$

$$\delta_O = \lambda_0 + \tfrac{3}{5}(qa)^2 \int_0^\infty dx\, x^3[1 - g(x)] + \mathcal{O}(q^4a^4)\,, \tag{5.26}$$

$$\delta_D = \lambda_D - \tfrac{1}{5}(qa)^2 \int_0^\infty dx\, x[1 - g(x)] + \mathcal{O}(q^4a^4)\,, \tag{5.27}$$

$$\delta_A = \lambda_A\,, \tag{5.28}$$

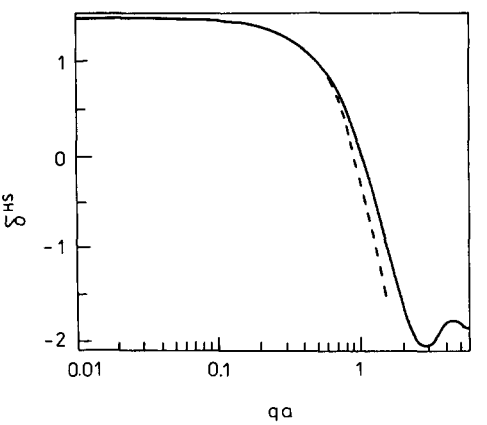

Fig. 5. Comparison of eq. (5.24) (dashed curve) with the exact numerical result of Russel and Glendinning [29] (full curve) for hard spheres.

$$\delta_S = \lambda_S - \tfrac{315}{448}(qa)^2 + \tfrac{45}{8}(qa)^2 \int_0^\infty dx\, x^{-3} g_1(x) + \mathcal{O}(q^4 a^4), \tag{5.29}$$

where $x = r/a$ is the dimensionless distance between the centers of the two particles. The expansion (5.29) can be performed only if $g_1(x)$ is decaying exponentially with x, because in the other cases the expansion is not convergent.

For strongly charged particles we must use the radial distribution function stemming from the perturbation treatment – see eqs. (2.5) and (2.13). In this case we obtain

$$\delta_i = \delta_i^{RHS} + \delta_i^{ELP}, \qquad i = V, O, A, D, S, \tag{5.30}$$

$$\delta_V^{RHS} = 8\gamma^3 - \tfrac{4}{5}p^2\gamma^5 + \tfrac{1}{35}p^4\gamma^7 + \mathcal{O}(p^6\gamma^9), \tag{5.31}$$

$$\delta_O^{RHS} = -6\gamma^2 + \tfrac{3}{5}p^2\gamma^4 - \tfrac{3}{140}p^4\gamma^6 + \mathcal{O}(p^6\gamma^8), \tag{5.32}$$

$$\delta_D^{RHS} = 1 - \tfrac{1}{10}p^2\gamma^2 + \tfrac{1}{280}p^4\gamma^4 + \mathcal{O}(p^6\gamma^6), \tag{5.33}$$

$$\delta_A^{RHS} = \lambda_A^{RHS} = -\tfrac{15}{8}\gamma^{-1} + \tfrac{9}{64}\gamma^{-3} + \mathcal{O}(\gamma^{-5}), \tag{5.34}$$

$$\delta_S^{RHS} = \tfrac{75}{256}\gamma^{-4} - \tfrac{315}{1792}p^2\gamma^{-2} + o(p^3). \tag{5.35}$$

These expansions are convergent only if $p\gamma^3 < 1$. Usually, for strongly charged particles and low or moderate electrolyte concentrations, $\gamma \geqslant 2$ (see fig. 1 and table I). One can estimate that, in this case, the effect of δ_D^{RHS}, δ_A^{RHS} and δ_S^{RHS} (i.e. near field hydrodynamics) can be neglected. Therefore, as a good approximation we obtain

$$\delta^{RHS} = 8\gamma^3 - 6\gamma^2 - (qa)^2\gamma^5 \frac{16}{5}\left(1 - \frac{3}{4\gamma}\right) + \mathcal{O}(q^4 a^4). \tag{5.36}$$

Sometimes the hydrodynamic term δ_O can be neglected in comparison with δ_V [3]. Eqs. (5.31) and (5.32) show that the contribution of δ_O^{RHS} can be neglected only if $\gamma \geqslant 10$, which corresponds to *high surface potentials and very small values of* κa (see fig. 1).

For δ_i^{ELP} we obtain

$$\delta_V^{ELP} = \lambda_V^{ELP} - (qa)^2 \frac{2W_0}{kT} \frac{e^{\kappa(2a-\sigma)}}{(\kappa a)^4} \left[\tfrac{1}{2}(\kappa\sigma)^3 + \tfrac{3}{2}(\kappa\sigma)^2 + 3\kappa\sigma + 3\right], \tag{5.37}$$

$$\delta_{\mathrm{O}}^{\mathrm{ELP}} = \lambda_{\mathrm{O}}^{\mathrm{ELP}} + \tfrac{6}{5}(qa)^2 \frac{2W_0}{kT} \frac{\mathrm{e}^{\kappa(2a-\sigma)}}{(\kappa a)^3} [\tfrac{1}{2}(\kappa\sigma)^2 + \kappa\sigma + 1], \tag{5.38}$$

$$\delta_{\mathrm{D}}^{\mathrm{ELP}} = 1 - \tfrac{1}{5}(qa)^2 \frac{2W_0}{kT} \mathrm{e}^{\kappa(2a-\sigma)} \frac{1}{\kappa a}, \tag{5.39}$$

$$\delta_{\mathrm{A}}^{\mathrm{ELP}} = \lambda_{\mathrm{A}}^{\mathrm{ELP}}, \tag{5.40}$$

$$\delta_{\mathrm{S}}^{\mathrm{ELP}} = \lambda_{\mathrm{S}}^{\mathrm{ELP}} + \tfrac{45}{8}(qa)^2 \frac{2W_0}{kT} \mathrm{e}^{2\kappa a} E_4(k\sigma) \frac{(\kappa a)^3}{(\kappa\sigma)^3}. \tag{5.41}$$

The numerical calculations show that $\delta_{\mathrm{S}}^{\mathrm{ELP}}$ and $\delta_{\mathrm{A}}^{\mathrm{ELP}}$ can be neglected in the sum of δ_i^{ELP}. λ_{D} can be also omitted in comparison with $\lambda_{\mathrm{V}}^{\mathrm{ELP}}$ and $\lambda_{\mathrm{O}}^{\mathrm{ELP}}$. Hence, we derive (see also eqs. (4.17) and (4.18))

$$\delta^{\mathrm{ELP}} = \lambda_{\mathrm{V}}^{\mathrm{ELP}} + \lambda_{\mathrm{O}}^{\mathrm{ELP}} + (qa)^2 \frac{2W_0}{kT} G(\kappa a, \kappa\sigma), \tag{5.42}$$

where

$$G(\kappa a, \kappa\sigma) = \frac{\mathrm{e}^{\kappa(2a-\sigma)}}{(\kappa a)^4} \{-[\tfrac{1}{2}(\kappa\sigma)^3 + \tfrac{3}{2}(\kappa\sigma)^2 + 3\kappa\sigma + 3] + \tfrac{6}{5}\kappa a[\tfrac{1}{2}(\kappa\sigma)^2 + \kappa\sigma + 1] - \tfrac{1}{5}(\kappa a)^3\}. \tag{5.43}$$

Eqs. (5.42), (5.43) together with eqs. (5.10), (5.30), and (5.36) determine the angular dependence of the effective diffusion coefficient in case of strongly charged particles.

For weakly charged particles, eqs. (5.25)–(5.29) lead to

$$\delta_i = \delta_i^{\mathrm{HS}} + \delta_i^{\mathrm{EL}}, \qquad i = \mathrm{V, O, A, D, S}, \tag{5.44}$$

where δ_i^{HS} has been determined above (see eqs. (5.19)–(5.23)), and δ_i^{EL} can be obtained from eqs. (5.37)–(5.41) by imposing $\sigma = 2a$ and W_0 given by eq. (2.25).

The final result is

$$\delta = \lambda^{\mathrm{HS}} + \lambda^{\mathrm{EL}} - 1.903(qa)^2 - (qa)^2 \frac{2W_0}{kT} \left(\frac{9}{5} \frac{1}{\kappa a} + \frac{18}{5} \frac{1}{(\kappa a)^2} + \frac{24}{5} \frac{1}{(\kappa a)^3} + \frac{3}{(\kappa a)^4} - \frac{45}{64} \exp(2\kappa a) E_4(2\kappa a) \right). \tag{5.45}$$

The numerical check shows that for not too large values of κa ($\kappa a < 2$) the

hard sphere contribution and the last term in the braces in eq. (5.45) can be omitted. The contribution of δ_D can be neglected only if $\kappa a \ll 1$.

Eqs. (5.25)–(5.29) show that the expansion of δ at small angles keeps only the even powers of qa. This fact can be used for the interpretation of DLS experimental data [18] (see section 6).

6. Dynamic light scattering experiments

The aim of this section is to demonstrate how the theoretical results, obtained above, can be used for interpretation of light scattering experiments.

The measurements were performed with three suspensions of different concentrations of latex particles in 2.25×10^{-4} mol/l NaCl. The radius of the particles was calculated by means of the Stokes–Einstein relation – see eq. (4.3). The diffusion coefficient $D_{SE} = 1.93 \times 10^{-7}$ cm^2/s, was measured at low latex concentration in excess of electrolyte (0.01 mol/l NaCl, $\phi = 5 \times 10^{-4}$) in order to avoid the influence of the particle interaction and the effect of the deformation of the counterion atmosphere [30, 31]. Thus, we obtained $a =$ 12.7 nm for the hydrodynamic radius of the particles. The volume fraction of the latex particles in the experiments was below 10^{-3}. So, we neglected the contribution of the counterions dissociated from the particles in the value of the screening parameter κ. Thus, κa was calculated to be equal to 0.632. As it is proved below, the surface potential of the particles is greater than 25 mV and the perturbation theory with nonlinear PBE is to be applied for interpretation of the results.

The equipment we used was a Malvern 4700C system (Malvern Ltd., England), supplied with a K7032 CE 8 Multibit correlator. The light source was an Argon laser (Innova 70, Coherent) operating at 488 nm wavelength of vertically plane polarized light. The temperature of the samples was automatically kept at 25 ± 0.1°C. Details for the sample preparation and measurements are described elsewhere [18].

For a given concentration of latex particles we measured the autocorrelation function $g^{(1)}(q, \tau)$ at different scattering angles. Using the first cumulant K_1 (cf. eq. (5.4)) we calculated the effective diffusion coefficient $D_{EFF}(q, \phi)$ from each $g^{(1)}(q, \tau)$ curve. In fig. 6 are shown the values of D_{EFF} (the points) determined in this way for three different latex volume fractions: $\phi = 3.33 \times 10^{-4}$, 6.67×10^{-4}, and 10.0×10^{-4}. Each of these three sets of data was fitted with a polynomial of the type (see eqs. (5.36) and (5.42) and ref. [18]):

$$D_{EFF}(q) = D_C + b_1(qa)^2 + b_2(qa)^4 , \tag{6.1}$$

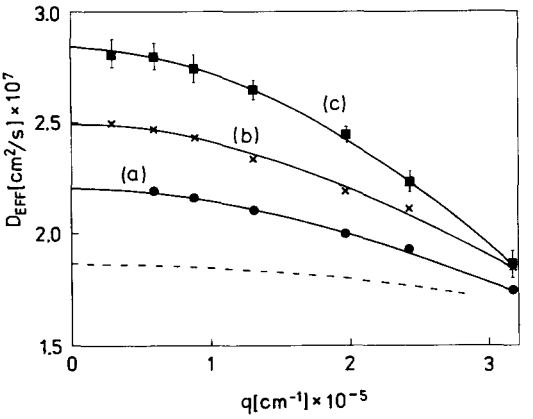

Fig. 6. Effective diffusion coefficient D_{EFF} versus the scattering vector q for charged polystyrene latex particles in 2.25×10^{-4} mol/l NaCl. The points are obtained by DLS measurements, and the curves are calculated by the least squares method (see eq. (6.1)): (a) $\phi = 3.3 \times 10^{-4}$; (b) $\phi = 6.7 \times 10^{-4}$; (c) $\phi = 10.0 \times 10^{-4}$. The dashed curve is obtained by linear extrapolation of D_{EFF} toward zero particle volume fraction at given q.

where the coefficients D_C, b_1 and b_2 were determined by means of the least squares method. The respective curves are shown in fig. 6 with full lines. The dashed curve in fig. 6 is obtained by linear extrapolation of D_{EFF} to zero particles concentration at a given scattering angle. It is briefly discussed at the end of this section, where the effects due to the finite diffusivity of the small ions on the particle diffusion and light scattering are considered. The values of D_C, and b_1 are summarized in table II. The higher the volume fraction ϕ, the higher the collective diffusion coefficient D_C. In accordance with eq. (4.1), from the slope of the plot of D_C versus ϕ we determined the interaction coefficient $\lambda = 520 \pm 20$. The intersect gives the single particle diffusion coefficient $D_0 = 1.86 \times 10^{-7}$ cm^2/s. The latter value is slightly lower than the value $D_{SE} = 1.93 \times 10^{-7}$ cm^2/s, which is due to the deformation of the electric double layer of the particles [18, 30, 31, 39]. The comparison of eq. (6.1) with eqs. (5.10), (5.36) and (5.42) shows that b_1 can be expressed in the following

Table II
Results for latex particles with radius $a = 12.7$ nm, $\kappa a = 0.632$. D_C and b_1 are determined from DLS experiments. b_1^* values are calculated for $W_0/kT = 110.5$. For more details see the explanations in the text. See also fig. 6.

ϕ (%)	$D_C \times 10^7$ (cm^2/s)	$b_1 \times 10^{12}$ (cm^2/s)	$b_1^* \times 10^{12}$ (cm^2/s)
0.033	2.20	−5.4	−5.0
0.067	2.44	−8.0	−10.0
0.100	2.84	−11.1	−15.0

manner:

$$b_1 = -D_0\phi\left[3.2\gamma^5\left(1-\frac{3}{4\gamma}\right)+2\,\frac{W_0}{kT}\,G(\kappa a,\,\kappa\sigma)\right]. \tag{6.2}$$

We have three experimental values for b_1 (table II) and one for λ, which must be fitted with uniform set of parameters. The problem can be divided into two consecutive parts:

(i) determination of parameter of interaction energy W_0. For that purpose we used the method of trials and errors to find the value of W_0 which corresponds to the experimentally obtained value of λ (or b_1) – see eqs. (4.22), (5.30), (5.36), (5.42), and (5.43). Besides, the value of γ and σ are evaluated using eqs. (2.9), (2.10), and (3.7);

(ii) calculation of the particle charge and potential from W_0. This was performed by numerical solution of the nonlinear PBE (2.14) together with the boundary conditions (2.17), and (2.18) (see also eq. (2.20)).

Using the above procedure and for $\lambda = 520$, $a = 12.7$ nm, and $\kappa a = 0.632$, we obtained the following values for some parameters of the system: $W_0/kT = 110.5$, $\sigma/a = 8.29$, $\gamma = 3.78$, $z_0 = 136.2$, and $e\Psi_s/kT = 3.82$. With these values of the parameters, we calculated the coefficients b_1^*. The results are shown in the last column of table II. The comparison with the measured value for b_1 evidences that the agreement is satisfactory. We should mention that the use of the linear theory (see eq. (4.12)) for such strongly charged colloidal particles leads to calculation of effective values for the particles charge and potential which are smaller than the real ones [18, 37, 40, 41]. For example, by introducing the same value for λ in the linear theory (eq. (4.12)) we obtain $z_0 = 45.6$ and $e\Psi_s/kT = 1.5$.

Some difficulties arise in the experimental investigations of systems of strongly charged particles, which are related to the high sensitivity of the results toward the value of κa. For example, the increase of κa with 10% may lead to a several times increase in the calculated z_0 and Ψ_s (cf. fig. 6 and table II). This means that small errors in κa may lead to large deviations of the calculated particle charge and potential from the actual values. The polydispersity of most of the real samples produces inevitable uncertainty for κa, used in the computations.

The coupling between the colloid–colloid, and colloid–small ions interactions was neglected in the present consideration. In principle it can be accounted for by using the coupled mode theory [40, 41]. It was shown by Belloni and Drifford [40] (see also ref. [18]) that the effect of the small ions on the coefficient λ is proportional to the ratio D_0/D_{SI} (D_{SI} is the small ion diffusion coefficient). Hence, it can be neglected in most cases.

Another question which can arise is whether the presence of small ions affects significantly the angular dependence of the effective diffusion coefficient $D_{EFF}(q)$. Considering our experiment (cf. the dashed line in fig. 6) we have not detected remarkable influence of the small ions.

7. Concluding remarks

In the present article, we have applied the perturbation statistical mechanical theory of Barker and Henderson [25] for determining the diffusion coefficient and sedimentation velocity of collodial particles. For this purpose, the equilibrium radial distribution function was split into two parts, corresponding to a reference system of effective hard spheres and to an electrostatic interaction perturbation. One should distinguish between this method and the effective hard sphere model which ascribes all charge effects to the effective particle excluded volume [3, 17]. The present article is a further development of our previous study [18], where a system of real hard spheres with low surface charge was examined.

By involving the theory of Felderhof [4, 10] into our considerations, we obtained analytical expressions for the first order correction of the diffusion coefficients and sedimentation velocity with respect to the volume fraction of particles (see eqs. (4.22)–(4.24)). The results were compared with exact numerical calculations, and also with the predictions of the EHS model (see fig. 3). Numerical results of other authors [23] were also used to check the accuracy, and range of validity of our model (see fig. 4 and table I).

The angular dependencies of the static and dynamic structure factors were examined. By introducing the perturbation approach into the general expressions given by Ackerson [36], and Pusey and Tough [3], we obtained analytical formulae for the static structure factor $S(q)$ (at arbitrary q), and dynamic structure factor $F(q, \tau)$ (at small q). They were compared with numerical calculations – see figs. 2 and 5.

The proposed theory (eqs. (3.6), (4.22)–(4.24)), (5.36) and (5.42)) allows the prediction of the diffusion coefficient and structure factors, if the particle size, charge, potential, ion concentration, and other parameters of the system are known. The equations we derived also give the opportunity to determine some of these parameters from light scattering experimental data. An illustration of such consideration is presented in fig. 6 and table II. From the measured by dynamic light scattering angular dependence of the effective diffusion coefficient $D_{EFF}(q)$, particle charge and potential have been calculated. We neglected the van der Waals attractive interaction in the present study because it is negligible for strongly charged particles at low concen-

trations of electrolyte. However, this interaction can be easily incorporated in our model.

Acknowledgements

We are indebted to Professor B.U. Felderhof for reading the first version of the manuscript and making some critical remarks, to Dr. P.A. Kralchevsky for the helpful discussions, and Mrs. R. Alargova for drawing the figures. This work was supported financially by the Bulgarian Ministry of Science and Higher Education.

References

[1] J.N. Israelachvili, Intermolecular and Surface Forces (Academic Press, London, 1985).
[2] C.A. Castillo, R. Rajagopalan and C.S. Hirtzel, Rev. Chem. Eng. 2 (1984) 239.
[3] P.N. Pusey and R.J.A. Tough, in: Dynamic Light Scattering, R. Pecora, ed. (Plenum, London, 1985).
[4] B.U. Felderhof, J. Phys. A 11 (1978) 929.
[5] G.K. Batchelor, J. Fluid Mech. 52 (1972) 245.
[6] G.K. Batchelor, J. Fluid Mech. 74 (1976) 1.
[7] W.B. Russel, D.A. Saville and W.R. Schowalter, Colloidal Dispersions (Cambridge Univ. Press, Cambridge, 1989).
[8] A. Einstein, Ann. Phys. 17 (1905) 549.
[9] B.U. Felderhof, Physica A 89 (1977) 373.
[10] B. Cichocki and B.U. Felderhof, J. Chem. Phys. 89 (1988) 1049.
[11] B. Cichocki, B.U. Felderhof and R. Schmitz, PhysicoChem. Hydrodyn. 10 (1988) 383.
[12] R.B. Jones and R. Schmitz, Physica A 149 (1988) 373.
[13] M.M. Kops-Werkhoven and H.M. Fijnaut, in: Light Scattering in Liquids and Macromolecular Solution, V. Degiorgio, M. Corti, and M. Giglio, eds. (Plenum, London, 1980).
[14] J. Newman, H.L. Swinney, S. Berkowtiz and L.A. Day, Biochemistry 13 (1974) 4832.
[15] R. Finsy, A. Devriese and H. Lekkerkerker, J. Chem. Soc. Farad. Trans. II 76 (1980) 767.
[16] T. Ohtsuki and K. Okano, J. Chem. Phys. 77 (1982) 1443.
[17] B. Cichocki and B.U. Felderhof, J. Chem. Phys. 94 (1991) 556.
[18] D.N. Petsev and N.D. Denkov, J. Colloid Interface Sci. (1992) in press.
[19] D.A. McQuarrie, Statistical Mechanics (Harper & Row, New York, 1976).
[20] B. Beresford-Smith, D.Y.C. Chan and D.J. Mitchell, J. Colloid Interf. Sci. 105 (1985) 216.
[21] J.B. Hayter and J. Penfold, Mol. Phys. 42 (1981) 109.
[22] J.-P. Hansen and J.B. Hayter, Mol. Phys. 46 (1982) 651.
[23] B. D'Aguanno, U. Genz and R. Klein, J. Phys.: Condens. Matter 2 (1990) 379.
[24] U. Genz and R. Klein, Physica A 171 (1991) 26.
[25] J.A. Barker and D. Henderson, Rev. Mod. Phys. 48 (1976) 587.
[26] J.A. Barker and D. Henderson, Ann. Rev. Phys. Chem. 23 (1972) 439.
[27] D. Levesque and L. Verlet, Phys. Rev. 182 (1969) 307.
[28] J.W. Goodwin and R.H. Ottewill, J. Chem. Soc. Farad. Trans. 87 (1991) 357.
[29] W.B. Russel and A.B. Glendinning, J. Chem. Phys. 74 (1981) 948.
[30] G.A. Schumacher and T.G.M. van de Ven, Faraday Discuss. Chem. Soc. 83 (1987) 75.

[31] G.A. Schumacher and T.G.M. van de Ven, J. Chem. Soc. Faraday Trans. 87 (1991) 971.
[32] R. Schmitz and B.U. Felderhof, Physica A 113 (1982) 90.
[33] R. Schmitz and B.U. Felderhof, Physica A 113 (1982) 103.
[34] R. Schmitz and B.U. Felderhof, Physica A 116 (1982) 163.
[35] J.L. Anderson, F. Rauh and A. Morales, J. Phys. Chem. 82 (1978) 608.
[36] B.J. Ackerson, J. Chem. Phys. 64 (1976) 242.
[37] S.-H. Chen and E.Y. Sheu, in: Micellar Solution and Microemulsions, S.-H. Chen and R. Rajagopalan, eds. (Springer, Berlin, 1990).
[38] P. Linse, J. Chem. Phys. 94 (1991) 3817.
[39] M. Medina-Noyola and A. Vizcarra-Rendon, Phys. Rev. A 32 (1985) 3596.
[40] L. Belloni and M. Drifford, J. Phys. (Paris) Lett. 46 (1985) 1183.
[41] M. Schurr, Chem. Phys. 111 (1987) 55.